A NOVEL ENERGY STORAGE ALLOCATION PLANNING METHOD FOR MICROGRID

by

Bin Chen

A Thesis Submitted in

Partial Fulfillment of the

Requirements for the Degree of

Master of Science

in Engineering

at

The University of Wisconsin-Milwaukee

May 2016

ABSTRACT

A NOVEL ENERGY STORAGE ALLOCATION PLANNING METHOD FOR MICROGRID

by

Bin Chen

The University of Wisconsin-Milwaukee, 2016
Under the Supervision of Professor David Yu

This paper proposes a novel energy storage system planning method with real time control. Sensitivity analysis is used to linearize the real power change in each certain generator brought by wind and ESS power change in system. Particle Swarm Optimization (PSO) is modified to include the real power change percentage as a constraint, and used to determine optimum ESS size and location. After extensive tests, it shows that this method can determine the optimum sizes and locations for ESS which can effectively keep the disturbance on generators in a system to the minimum while maintaining an acceptable system voltage profile after a sudden wind power drop.

TABLE OF CONTENTS

1 Introduction....1
2 Sensitivity Analysis in Power System....3
2.1 Newton-Raphson Fully Coupled Method....4
2.2 Sensitivity Analysis in Power System....8
2.3 Modeling Sudden Generator Output Variation....8
3 Particle Swarm Optimization....11
3.1 Algorithm PSO....11
3.2 Modified PSO for ESS Planning Integrating Generator Control....12
3.2.1 Algorithm PSO for ESS Planning Problem....13
3.2.2 Flow Chart:....14
4 Searching Space Reduction....16
4.1 Candidate Bus from Voltage Deviation Constraint....17
4.2 Candidate Bus from Generator Control Constraint....19
5 Case Study....21
5.1 Contrast with Other Method....24
5.2 Impact of Generator Location....26
5.2.1 Generator in bus 6....26
5.2.2 Generator in Bus 10....28
5.2.3 Generator in Bus 1 and Bus 6....31
6 Verification of the Proposed Algorithm....34
7 Conclusion and Future Work....36
8 References....37

1 Introduction

Wind energy industry has seen a cumulative growth rate of around 26% for the past eighteen years. The total wind power capacity is expected to reach nearly 2000 GW by 2030 in an advanced scenario, and to supply between 16.7% and 18.8% of global electricity demand [1]. However, a high penetration of wind power raises a problem of system instability, caused by the nature of wind uncertainty. Therefore, in many cases, wind turbine is working in conjunction with energy storage system (ESS), which can be used as a power and energy buffer, and effectively smooth the power output fluctuations [2].

Many studies have already shown the importance of optimal ESS allocation planning in wind energy penetrated system. Reference [3] discretizes wind power distribution by 5-point estimation method (5PEM), and combines Multi-Objective Particle Swarm Optimization (MOPSO) algorithm with elitist non-dominated sorting genetic algorithm (NSGA-II) to determine the optimal location and size of an energy storage system (ESS). Results prove more reasonable than worst case (zero wind) planning, for this method can minimize the total operation cost and improve voltage profiles. Reference [4] includes random forecast error of wind power into the proposed formulation by using a scenario tree model, and applies Benders decomposition algorithm to reduce the computational burden. Reference [5] proposes an analytical technique to size ESS for power systems with wind farms based on reliability cost and worth analysis, which can provide useful information for power system planners or wind farm owners to make decisions for system expansion.

However, these planning methods are all focused on steady state planning which do not consider about the transient control part of system when wind power changes. In many cases,

control may not be able to handle of the optimally designed ESS system, especially when wind power drops suddenly.

A sudden wind power drop will cause the unbalance between generation and consumption in a system. To make up for this power deficiency, generators should output more real power. Obviously, it will be difficult for generator to react if there is a large real power change.

ESS working in conjunction with the generators can instantaneously produce more real power to supplement the lost wind power and reduce the stress on generators. ESS's size and location will be the importance factors. In ESS allocation planning, if this generator control part can be taken into consideration, the results can not only help alleviate the negative effects caused by the sudden wind drop, but it will also help the generators to have smoother response to the sudden wind drop.

In this thesis, sensitivity analysis [6] is used to linearize the real power change in a certain generator brought by wind and ESS power fluctuation. Particle Swarm Optimization (PSO) is modified to include the real power change percentage as a constraint, and used to determine optimum ESS size and location.

2 Sensitivity Analysis in Power System

Power flow (load flow) is of great importance in planning and designing the future expansion of power systems as well as in determining the best operation of existing systems. The principle information obtained from a power flow study is the magnitude and phase angle of the voltage at each bus and the real and reactive power flow in each line [7].

In short, what power flow does is to solve the following complex matrix equation (2.1) and obtain angle and voltage magnitude in every bus.

$$YV = I = \frac{S^*}{V^*} \tag{2.1}$$

Y is the network nodal admittance matrix, V is the unknown complex node voltage vector, I is the nodal current injection vector, and S = P+ jQ is the apparent power nodal injection vector that represents the specified load and the generation at demand or generation nodes respectively.

However, power flow equation is not as simple as what it looks like, for it is a non-linear equation, which has to be solved using a non-linear method to find the value of the unknowns. There are methods such as Gauss-Seidel, Newton-Raphson and Newton-Raphson decoupled [8]; each one of the methods has certain advantages and disadvantages for solving the power flow.

In the power flow solution technique, a three phase bus can be classified according to the following table:

Table 2.1

BUS TYPE	UNKNOWNS
PQ	The complex node voltage
PV	Reactive power Q and voltage phase δ
Swing Bus	Infinite source, active P and reactive Q are unknown

2.1 Newton-Raphson Fully Coupled Method

This method is considered the most general and reliable method to solve the power flow equations. Once the equations for the power flow have been defined, the solution algorithm involves iteration based on successive linearization using the first term of a Taylor series expansion of the equations to be solved [6].

First of all, the power flow equation using the power injected at node i, can be written as:

$$P_i - jQ_i = V_i^* \sum_{k=1}^{n} Y_{ik} V_k \tag{2.2}$$

where,

$$Y_{ik} = |Y_{ik}| \angle \theta_{ik} \tag{2.3}$$

$$V_k = |V_k| \angle \delta_k \tag{2.4}$$

$$V_i = |V_i| \angle \delta_i \tag{2.5}$$

Therefore, substituting equations (2.3)-(2.5) into equation (2.2), equation (2.6) is obtained.

$$P_i - jQ_i = \sum_{k=1}^{n} |Y_{ik}||V_k||V_i| \angle (\theta_{ik} - \delta_i + \delta_k) \tag{2.6}$$

From equation (2.6), active and reactive power can be separately calculated as:

$$P_i = \sum_{k=1}^{n} |Y_{ik}||V_k||V_i| \cos(\theta_{ik} - \delta_i + \delta_k) \tag{2.7}$$

$$Q_i = -\sum_{k=1}^{n} |Y_{ik}||V_k||V_i| \sin(\theta_{ik} - \delta_i + \delta_k) \tag{2.8}$$

Rearranging equation (2.7) and equation (2.8), the specified variable can be differentiated from the variable that is to be calculated, as shown in equation (2.9) and equation (2.10).

$$\{P_i\} - \sum_{k=1}^{n} |Y_{ik}||V_k||V_i| \cos(\theta_{ik} - \delta_i + \delta_k) = 0 \tag{2.9}$$

$$\{Q_i\} + \sum_{k=1}^{n} |Y_{ik}||V_k||V_i| \sin(\theta_{ik} - \delta_i + \delta_k) = 0 \tag{2.10}$$

where,

P_i and Q_i are the specific variables. $\sum_{k=1}^{n} |Y_{ik}||V_k||V_i| \cos(\theta_{ik} - \delta_i + \delta_k)$ and $\sum_{k=1}^{n} |Y_{ik}||V_k||V_i| \sin(\theta_{ik} - \delta_i + \delta_k)$ are the variables to calculate.

$$P_i = P_{ig} - P_{id} \tag{2.11}$$

$$Q_i = Q_{ig} - Q_{id} \tag{2.12}$$

where,

P_{ig} is the scheduled real power being generated at bus i, P_{id} is the scheduled real power demand of the load at bus i.

Q_{ig} is the scheduled reactive power being generated at bus i, Q_{id} is the scheduled reactive power demand of the load at bus i.

There are some important observations from equation (2.7) and (2.8). If the bus is a slack bus, neither equation (2.7) nor (2.8) exists. If the type of bus is a PQ bus, both equations exists. If the bus is a PV bus only equation (2.7) will exist in the solution of the method.

To solve equation (2.9) and (2.10), Taylor series expansion is used. As mentioned before, only the first partial derivatives are considered.

If Taylor series expansion is expressed in matrix equation, Jacobian Matrix will be obtained. Assuming Bus 1 is the swing bus, for n buses system, the Taylor series expansion and Jacobian Matrix will have the following form:

$$\begin{bmatrix} \Delta P_2 \\ \Delta P_3 \\ \vdots \\ \vdots \\ \Delta P_n \\ \Delta Q_2 \\ \Delta Q_3 \\ \vdots \\ \vdots \\ \Delta Q_n \end{bmatrix} = \begin{bmatrix} \frac{\partial P_2}{\partial \delta_2} & \frac{\partial P_2}{\partial \delta_3} & \cdots & \frac{\partial P_2}{\partial \delta_n} & \frac{\partial P_2}{\partial |V_2|} & \frac{\partial P_2}{\partial |V_3|} & \cdots & \frac{\partial P_2}{\partial |V_n|} \\ \frac{\partial P_3}{\partial \delta_2} & \frac{\partial P_3}{\partial \delta_3} & \cdots & \frac{\partial P_3}{\partial \delta_n} & \frac{\partial P_3}{\partial |V_2|} & \frac{\partial P_3}{\partial |V_3|} & \cdots & \frac{\partial P_3}{\partial |V_n|} \\ \vdots & \vdots & \vdots & \vdots & \vdots & \vdots & \vdots & \vdots \\ \frac{\partial P_n}{\partial \delta_2} & \frac{\partial P_n}{\partial \delta_3} & \cdots & \frac{\partial P_n}{\partial \delta_n} & \frac{\partial P_n}{\partial |V_2|} & \frac{\partial P_n}{\partial |V_3|} & \cdots & \frac{\partial P_n}{\partial |V_n|} \\ \frac{\partial Q_2}{\partial \delta_2} & \frac{\partial Q_2}{\partial \delta_3} & \cdots & \frac{\partial Q_2}{\partial \delta_n} & \frac{\partial Q_2}{\partial |V_2|} & \frac{\partial Q_2}{\partial |V_3|} & \cdots & \frac{\partial Q_2}{\partial |V_n|} \\ \frac{\partial Q_3}{\partial \delta_2} & \frac{\partial Q_3}{\partial \delta_3} & \cdots & \frac{\partial Q_3}{\partial \delta_n} & \frac{\partial Q_3}{\partial |V_2|} & \frac{\partial Q_3}{\partial |V_3|} & \cdots & \frac{\partial Q_3}{\partial |V_n|} \\ \vdots & \vdots & \vdots & \vdots & \vdots & \vdots & \vdots & \vdots \\ \frac{\partial Q_n}{\partial \delta_2} & \frac{\partial Q_n}{\partial \delta_3} & \cdots & \frac{\partial Q_n}{\partial \delta_n} & \frac{\partial Q_n}{\partial |V_2|} & \frac{\partial Q_n}{\partial |V_3|} & \cdots & \frac{\partial Q_n}{\partial |V_n|} \end{bmatrix} \begin{bmatrix} \Delta \delta_2 \\ \Delta \delta_3 \\ \vdots \\ \vdots \\ \Delta \delta_n \\ \Delta |V_2| \\ \Delta |V_3| \\ \vdots \\ \vdots \\ \Delta |V_n| \end{bmatrix} \quad (2.13)[6]$$

$$\begin{bmatrix} \frac{\partial P_2}{\partial \delta_2} & \frac{\partial P_2}{\partial \delta_3} & \cdots & \frac{\partial P_2}{\partial \delta_n} & \frac{\partial P_2}{\partial |V_2|} & \frac{\partial P_2}{\partial |V_3|} & \cdots & \frac{\partial P_2}{\partial |V_n|} \\ \frac{\partial P_3}{\partial \delta_2} & \frac{\partial P_3}{\partial \delta_3} & \cdots & \frac{\partial P_3}{\partial \delta_n} & \frac{\partial P_3}{\partial |V_2|} & \frac{\partial P_3}{\partial |V_3|} & \cdots & \frac{\partial P_3}{\partial |V_n|} \\ \vdots & \vdots & \vdots & \vdots & \vdots & \vdots & \vdots & \vdots \\ \frac{\partial P_n}{\partial \delta_2} & \frac{\partial P_n}{\partial \delta_3} & \cdots & \frac{\partial P_n}{\partial \delta_n} & \frac{\partial P_n}{\partial |V_2|} & \frac{\partial P_n}{\partial |V_3|} & \cdots & \frac{\partial P_n}{\partial |V_n|} \\ \frac{\partial Q_2}{\partial \delta_2} & \frac{\partial Q_2}{\partial \delta_3} & \cdots & \frac{\partial Q_2}{\partial \delta_n} & \frac{\partial Q_2}{\partial |V_2|} & \frac{\partial Q_2}{\partial |V_3|} & \cdots & \frac{\partial Q_2}{\partial |V_n|} \\ \frac{\partial Q_3}{\partial \delta_2} & \frac{\partial Q_3}{\partial \delta_3} & \cdots & \frac{\partial Q_3}{\partial \delta_n} & \frac{\partial Q_3}{\partial |V_2|} & \frac{\partial Q_3}{\partial |V_3|} & \cdots & \frac{\partial Q_3}{\partial |V_n|} \\ \vdots & \vdots & \vdots & \vdots & \vdots & \vdots & \vdots & \vdots \\ \frac{\partial Q_n}{\partial \delta_2} & \frac{\partial Q_n}{\partial \delta_3} & \cdots & \frac{\partial Q_n}{\partial \delta_n} & \frac{\partial Q_n}{\partial |V_2|} & \frac{\partial Q_n}{\partial |V_3|} & \cdots & \frac{\partial Q_n}{\partial |V_n|} \end{bmatrix} \quad (2.14)$$

Jacobian Matrix (2.14) can be divided into four parts J_{11}, J_{12}, J_{21}, J_{22}, which have different physical meaning.

$$J_{11} = \frac{\partial P}{\partial \delta} = \begin{bmatrix} \frac{\partial P_2}{\partial \delta_2} & \frac{\partial P_2}{\partial \delta_3} & \cdots & \frac{\partial P_2}{\partial \delta_n} \\ \frac{\partial P_3}{\partial \delta_2} & \frac{\partial P_3}{\partial \delta_3} & \cdots & \frac{\partial P_3}{\partial \delta_n} \\ \vdots & \vdots & \vdots & \vdots \\ \frac{\partial P_n}{\partial \delta_2} & \frac{\partial P_n}{\partial \delta_3} & \cdots & \frac{\partial P_n}{\partial \delta_n} \end{bmatrix} \tag{2.15}$$

$$J_{12} = \frac{\partial P}{\partial |V|} = \begin{bmatrix} \frac{\partial P_2}{\partial |V_2|} & \frac{\partial P_2}{\partial |V_3|} & \cdots & \frac{\partial P_2}{\partial |V_n|} \\ \frac{\partial P_3}{\partial |V_2|} & \frac{\partial P_3}{\partial |V_3|} & \cdots & \frac{\partial P_3}{\partial |V_n|} \\ \vdots & \vdots & \vdots & \vdots \\ \frac{\partial P_n}{\partial |V_2|} & \frac{\partial P_n}{\partial |V_3|} & \cdots & \frac{\partial P_n}{\partial |V_n|} \end{bmatrix} \tag{2.16}$$

$$J_{21} = \frac{\partial Q}{\partial \delta} = \begin{bmatrix} \frac{\partial Q_2}{\partial \delta_2} & \frac{\partial Q_2}{\partial \delta_3} & \cdots & \frac{\partial Q_2}{\partial \delta_n} \\ \frac{\partial Q_3}{\partial \delta_2} & \frac{\partial Q_3}{\partial \delta_3} & \cdots & \frac{\partial Q_3}{\partial \delta_n} \\ \vdots & \vdots & \vdots & \vdots \\ \frac{\partial Q_n}{\partial \delta_2} & \frac{\partial Q_n}{\partial \delta_3} & \cdots & \frac{\partial Q_n}{\partial \delta_n} \end{bmatrix} \tag{2.17}$$

$$J_{22} = \frac{\partial Q}{\partial |V|} = \begin{bmatrix} \frac{\partial Q_2}{\partial |V_2|} & \frac{\partial Q_2}{\partial |V_3|} & \cdots & \frac{\partial Q_2}{\partial |V_n|} \\ \frac{\partial Q_3}{\partial |V_2|} & \frac{\partial Q_3}{\partial |V_3|} & \cdots & \frac{\partial Q_3}{\partial |V_n|} \\ \vdots & \vdots & \vdots & \vdots \\ \frac{\partial Q_n}{\partial |V_2|} & \frac{\partial Q_n}{\partial |V_3|} & \cdots & \frac{\partial Q_n}{\partial |V_n|} \end{bmatrix} \tag{2.18}$$

Based on equation (2.15)-(2.18), (2.13) can be rewritten as

$$\begin{bmatrix} \Delta P \\ \Delta Q \end{bmatrix} = \begin{bmatrix} \frac{\partial P}{\partial \delta} & \frac{\partial P}{\partial |V|} \\ \frac{\partial Q}{\partial \delta} & \frac{\partial Q}{\partial |V|} \end{bmatrix} \begin{bmatrix} \Delta \delta \\ \Delta |V| \end{bmatrix} \tag{2.19}$$

2.2 Sensitivity Analysis in Power System

Once the power system steady state has been calculated by solving power non-linear equations. The inverse of the Jacobian Matrix can also be obtained, and the inverse will have the structure as follows.

$$\begin{bmatrix} \frac{\partial \delta_2}{\partial P_2} & \frac{\partial \delta_2}{\partial P_3} & \cdots & \frac{\partial \delta_2}{\partial P_n} & \frac{\partial \delta_2}{\partial Q_2} & \frac{\partial \delta_2}{\partial Q_3} & \cdots & \frac{\partial \delta_2}{\partial Q_n} \\ \frac{\partial \delta_3}{\partial P_2} & \frac{\partial \delta_3}{\partial P_3} & \cdots & \frac{\partial \delta_3}{\partial P_n} & \frac{\partial \delta_3}{\partial Q_2} & \frac{\partial \delta_3}{\partial Q_3} & \cdots & \frac{\partial \delta_3}{\partial Q_n} \\ \vdots & \vdots & \vdots & \vdots & \vdots & \vdots & \vdots & \vdots \\ \frac{\partial \delta_n}{\partial P_2} & \frac{\partial \delta_n}{\partial P_3} & \cdots & \frac{\partial \delta_n}{\partial P_n} & \frac{\partial \delta_n}{\partial Q_2} & \frac{\partial \delta_n}{\partial Q_3} & \cdots & \frac{\partial \delta_n}{\partial Q_n} \\ \frac{\partial |V_2|}{\partial P_2} & \frac{\partial |V_2|}{\partial P_3} & \cdots & \frac{\partial |V_2|}{\partial P_n} & \frac{\partial |V_2|}{\partial Q_2} & \frac{\partial |V_2|}{\partial Q_3} & \cdots & \frac{\partial |V_2|}{\partial Q_n} \\ \frac{\partial |V_3|}{\partial P_2} & \frac{\partial |V_3|}{\partial P_3} & \cdots & \frac{\partial |V_3|}{\partial P_n} & \frac{\partial |V_3|}{\partial Q_2} & \frac{\partial |V_3|}{\partial Q_3} & \cdots & \frac{\partial |V_3|}{\partial Q_n} \\ \vdots & \vdots & \vdots & \vdots & \vdots & \vdots & \vdots & \vdots \\ \frac{\partial |V_n|}{\partial P_2} & \frac{\partial |V_n|}{\partial P_3} & \cdots & \frac{\partial |V_n|}{\partial P_n} & \frac{\partial |V_n|}{\partial Q_2} & \frac{\partial |V_n|}{\partial Q_3} & \cdots & \frac{\partial |V_n|}{\partial Q_n} \end{bmatrix} \begin{bmatrix} \Delta P_2 \\ \Delta P_3 \\ \vdots \\ \vdots \\ \Delta P_n \\ \Delta Q_2 \\ \Delta Q_3 \\ \vdots \\ \vdots \\ \Delta Q_n \end{bmatrix} = \begin{bmatrix} \Delta \delta_2 \\ \Delta \delta_3 \\ \vdots \\ \vdots \\ \Delta \delta_n \\ \Delta |V_2| \\ \Delta |V_3| \\ \vdots \\ \vdots \\ \Delta |V_n| \end{bmatrix} \quad (2.20)$$

Inverse of Jacobian Matrix can be written as $[J]^{-1}$, which is called Sensitivity Matrix [6]. This matrix basically describes the impact on the voltage magnitude and angle of each bus, due to a change in active/reactive power at some particular location.

2.3 Modeling Sudden Generator Output Variation

Assuming there is suddenly a wind power change in wind farm, it will cause the unbalance between generation and consumption because consumption in system does not change instantly. Generators should output more real power to make up for this power deficiency. However,

sudden real power change in generators will bring large disturbing, even instability for generators. As the other real power source in system, ESS will instantaneously output more real power to supplement the lost wind power and reduce the stress on generators

Sensitivity matrix can basically describe the impact on all buses due to a change in active/reactive power at some particular location. Therefore, sensitivity analysis equation (2.21) can be used to calculate when wind power changes and ESS reacts, how the angle and voltage magnitude will change in power system.

$$\left[J\right]^{-1}\begin{bmatrix} \vdots \\ \Delta \mathrm{P}_{w} \\ \vdots \\ \Delta \mathrm{P}_{ESS1} \\ \vdots \\ \Delta \mathrm{P}_{ESS2} \\ \vdots \\ 0 \\ 0 \\ \vdots \\ 0 \\ 0 \\ \vdots \\ \vdots \end{bmatrix} = \begin{bmatrix} \Delta\delta_2 \\ \Delta\delta_3 \\ \Delta\delta_4 \\ \Delta\delta_5 \\ \vdots \\ \vdots \\ \vdots \\ \Delta|V_2| \\ \Delta|V_3| \\ \Delta|V_4| \\ \Delta|V_5| \\ \vdots \\ \vdots \\ \vdots \end{bmatrix} \tag{2.21}$$

$\Delta \mathrm{P}_{w}$ is the real power change in wind power bus, and $\Delta \mathrm{P}_{ESS}$ is the real power change in ESS bus. After voltage angle and magnitude change in system are calculated, these variables can be substituted into the equation (2.22).

Equation (2.22) can be used to calculate real power change in any bus of this system.

$$\begin{aligned} \Delta P_i = {} & \frac{\partial P_i}{\partial \delta_1}\Delta\delta_1 + \frac{\partial P_i}{\partial \delta_2}\Delta\delta_2 + \frac{\partial P_i}{\partial \delta_3}\Delta\delta_3 + \cdots \frac{\partial P_i}{\partial |V_1|}\Delta|V_1| \\ & + \frac{\partial P_i}{\partial |V_2|}\Delta|V_2| + \frac{\partial P_i}{\partial |V_3|}\Delta|V_3| + \cdots \end{aligned} \tag{2.22}$$

Because bus 1 is the swing bus, so in equation (2.22) $\Delta\delta_1 = \Delta V_1 = 0$. Also, all PV bus's voltage magnitude should be set to 0.

Using equation (2.22), every generator bus' real power change can be calculated. Since disturbing to a certain generator is also associated with its power size, index β can be used to describe the severity of wind power change on the generator.

$$\beta = \Delta P_i / P_{irate}$$

Where ΔP_i is the real power change in bus i, and P_{irate} is the rated power of generator i. If $|\beta|$ is larger than the maximum real power change percentage of generator, it means generator suffers too much disturbing, which may cause instability of the generator.

In the following chapter, algorithm PSO is modified to include β as a constraint, which proves effectively to help alleviate the negative effects on generators caused by the sudden wind power change.

3 Particle Swarm Optimization

3.1 Algorithm PSO

The PSO is a swarm intelligence method inspired by social behavior of bird flocking or fish schooling ,developed for global optimization algorithm by J.Kennady and R.Eberhart in 1995 [9]. It has become one of the most popular techniques for various optimization problems due to its easiness and capability to find near optimal solutions. The PSO uses a number of particles that constitute a swarm. Each particle traverses the search space looking for the global optimal (minimum or maximum). In a PSO system, particles fly round in a multidimensional search space. During flight, each particle regulates its position according to its own experience, and the experience of neighboring particles, making use of the best position encountered by itself and its neighbors.

The main advantages of the PSO method [10]:

1) Faster performance than other meta-heuristic search methods.

2) Faster convergence and fewer number of control parameters.

3) More powerful search ability.

4) Easy handling of integer and discrete optimization,

5) Simple in coding and easy to use.

In the PSO method, the movement of each particle in the population is determined via its location (particle coordinates x) and velocity (flight speed v). During the movement, the velocity of particles is changed over time and their position will be updated consequently. For instance, in a N-dimension optimization problem, the position and velocity vectors of particle

i are represented by $x_i = [x_{i1}, x_{i2}, x_{i3} \cdots x_{iN}]$ and $v_i = [v_{i1}, v_{i2}, v_{i3} \cdots v_{iN}]$, respectively. The best previous position of particle i is based on the value of fitness function represented by $pbest_i = [x_{i1}^{pbest}, x_{i2}^{pbest}, x_{i3}^{pbest} \cdots x_{iN}^{pbest}]$ and the best particle among all particles represented by gbest. The modified velocity and position of each particle can be calculated as shown in the following formulation:

$$v_i^{k+1} = wv_i^k + c_1 r_1 (pbest_i^k - x_i^k) + c_2 r_2 (gbest^k - x_i^k) \quad (3.1)$$

$$x_i^{k+1} = x_i^k + v_i^{k+1} \quad (3.2)$$

where,

w the inertia weight;

c_1 *and* c_2 acceleration constants;

r_1 *and* r_2 two random numbers in the range of [0, 1];

$pbest_i^k$ the best position particle i achieved based on its own experience,

$pbest_i^k = [x_{i1}^{pbest}, x_{i2}^{pbest}, x_{i3}^{pbest}, \cdots x_{iN}^{pbest}]$;

$gbest^k$ the best particle position based on overall swarm's experience,

$gbest^k = [x_1^{gbest}, x_2^{gbest}, x_3^{gbest}, \cdots x_N^{gbest}]$;

In order to improve the efficiency and accuracy, a linearly decreasing inertia weight from maximum $w_{\max}$ to minimum $w_{\min}$ is applied to update the inertia weight:

$$w^k = w_{\max} - \frac{w_{\max} - w_{\min}}{k_{\max}} \cdot k \quad (3.3)$$

where $w_{\max}$ and $w_{\min}$ are the initial and final inertia weights, $k_{\max}$ is the maximum iteration number [11].

3.2 Modified PSO for ESS Planning Integrating Generator Control

In this algorithm, every scenario of allocating ESS in power system can be represented by a

particle. For example, if n ESS are planned to be located in N bus system, and there are m particles, then the position of particle i can be written as $x_i = [x_{i1}, x_{i2}, x_{i3} \cdots x_{in}]$, where x_{in} represents ESS size in the corresponding bus. The fitness value of particle i is the ESS total size it represents, which means,

$$Fitness\ value(i) = \sum_{j=1}^{n} \left| x_{ij} \right| \tag{3.4}$$

Objective function:

$$\min\ f = \sum_{j=1}^{n} \left| x_j \right| \tag{3.5}$$

Two constraints:

Voltage deviation constraint:

$$\alpha = \sqrt{\sum_{j=1}^{N} (\left| V_j \right| - \left| V_{jref} \right|)^2} \tag{3.6}$$

Generator control constraint:

$$\beta = \Delta P_j / P_{jrate} \tag{3.7}$$

3.2.1 Algorithm PSO for ESS Planning Problem

Step1. Randomly select n buses from a N bus system to locate ESS.

Step2. Generate m particles. Each particle is 1 row and n column. The number in each column is ESS's size in corresponding bus. Initialize particles' velocity, Pbest and Gbest.

Step3. Update each particle's velocity and position using equation (3.1) and (3.2).

Step4. For particle i, calculate the voltage deviation α. If it exceeds constrains, regenerate one new particle, and calculate the voltage deviation again, till it satisfies the voltage constraint.

Step5. For particle i, calculate index β in a certain generator bus, when wind power suddenly

drops, and ESS reacts instantaneously. If index β exceeds constrains, regenerate one new particle, and calculate the disturbing again, till it satisfies the control constraint.

Step6. If particle i satisfies both constraints, its fitness value can be calculated. If it is smaller than pbest, pbest can be replaced by the position of particle i.

Step7. Redo step 3~6 on the rest particles. Then choose the minimum pbest to be gbest.

Step8. After 30 iterations, choose the best particle from the last iteration. This particle will satisfy all the constraint and be the minimum ESS cost one.

3.2.2 Flow Chart:

The flow chart of the proposed method is shown in figure 3.1

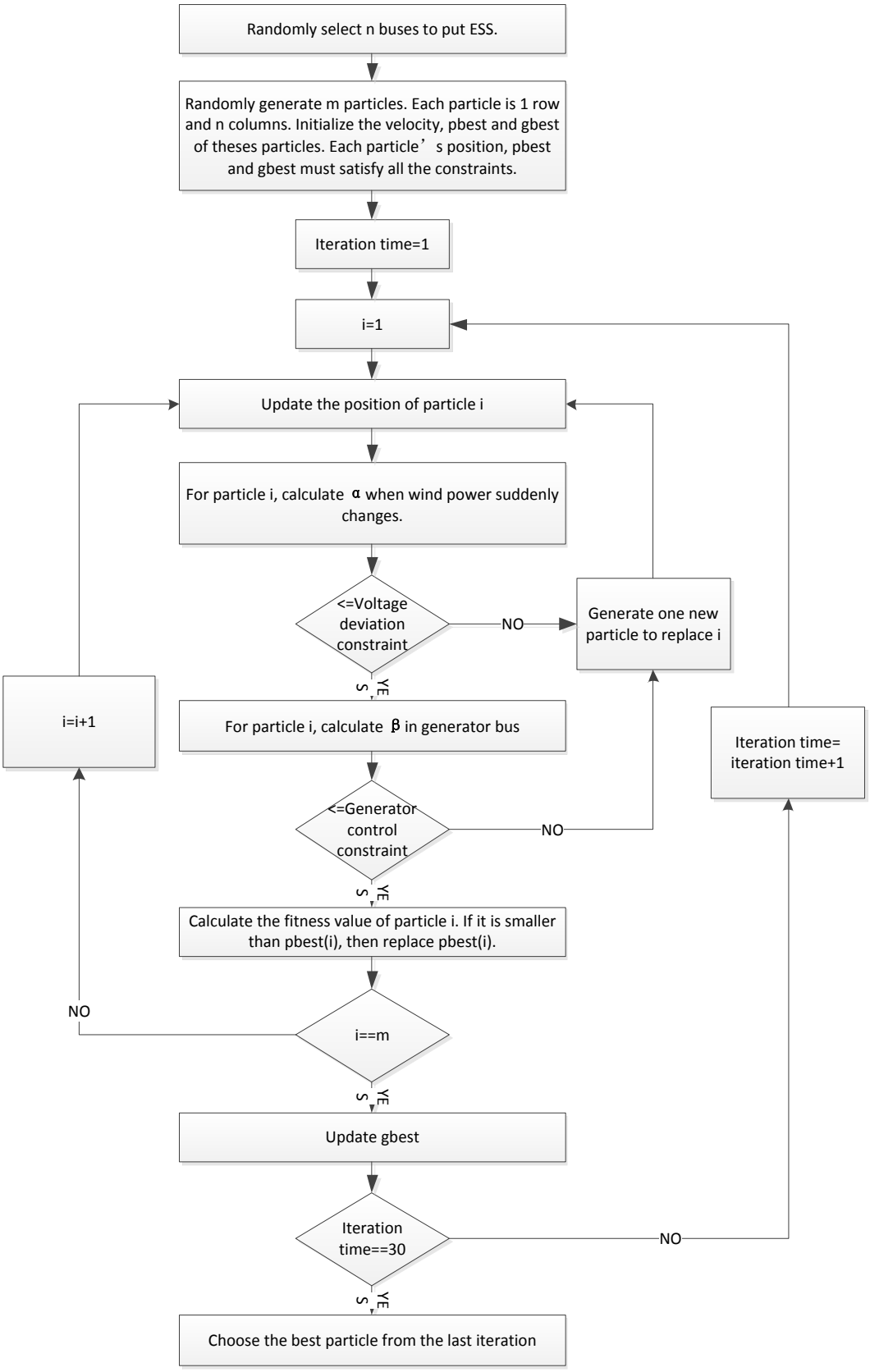

Figure 3.1 flow chart

4 Searching Space Reduction

As is explained in chapter 3, modified PSO will firstly select n bus from N bus system, and then optimize ESS size. However, if it is a large and complex system, there may be a lot of possibilities of bus combination. If optimization covers all the buses, program will take a long time. Therefore, it is necessary to reduce algorithm searching space and small amount of candidate bus is needed. PSO program will then only select ESS bus from candidate bus instead of the whole system, which can reduce the calculation cost to a large extent.

Using IEEE 30 System as an example.

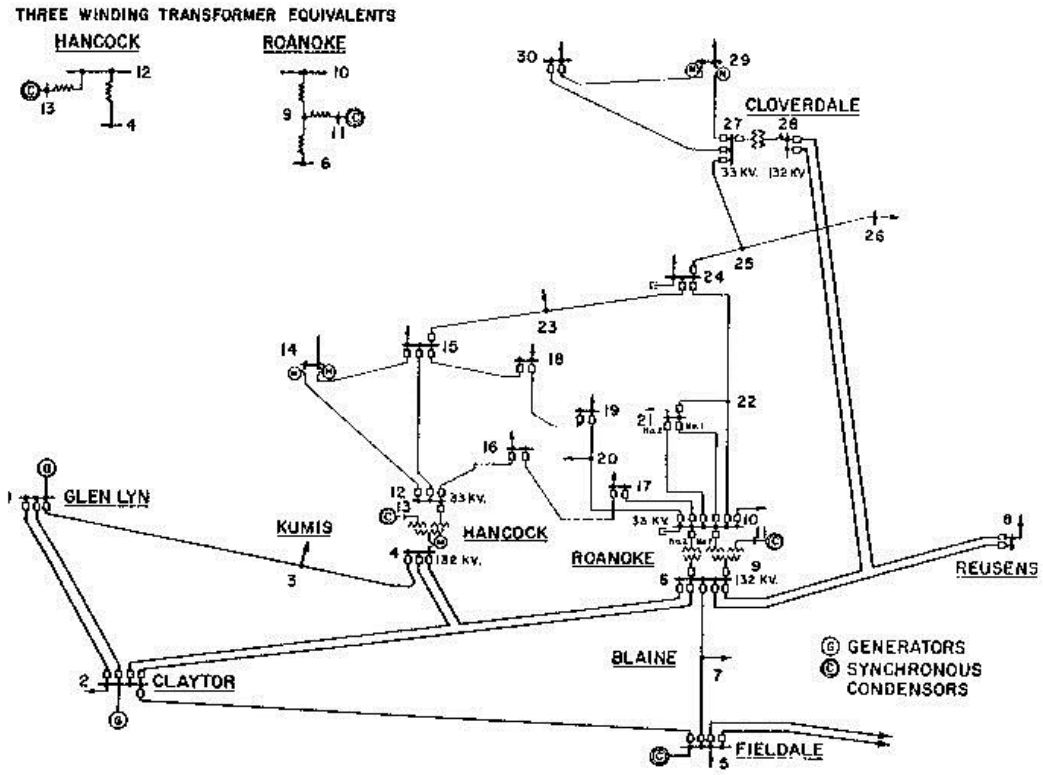

Figure 4.1 IEEE 30 system [12]

There are two constraints in optimization, one is voltage deviation constraint and the other is generator control constraint. These two constraint can be used to determine candidate bus.

4.1 **Candidate Bus from Voltage Deviation Constraint**

Wind drop can cause a significant voltage angle and magnitude change in system. As mentioned before, the voltage deviation in the system can be expressed as

$$\alpha = \sqrt{\sum_{j=1}^{N} (|V_j| - |V_{jref}|)^2} \tag{4.1}$$

Where V_j is the actual voltage in bus j, and V_{jref} is the reference voltage in bus j.

To satisfy the voltage deviation constraint and reduce the total size, ESS should be located in buses whose power change can significantly influence system's voltage. As mentioned before, sensitivity matrix can basically describe the impact in all different locations, due to a change in active/reactive power at some particular location. Therefore, some index can be applied based on sensitivity matrix.

$$Index_{1j} = \sum_{i=1}^{N} \left| \frac{\partial \delta_i}{\partial P_j} \right| \tag{4.2}$$

$$Index_{2j} = \sum_{i=1}^{N} \left| \frac{\partial \delta_i}{\partial Q_j} \right| \tag{4.3}$$

$$Index_{3j} = \sum_{i=1}^{N} \left| \frac{\partial |V_i|}{\partial P_j} \right| \tag{4.4}$$

$$Index_{4j} = \sum_{i=1}^{N} \left| \frac{\partial |V_i|}{\partial Q_j} \right| \tag{4.5}$$

Since our focus is on real power, only $Index_1$ and $Index_3$ are needed. Buses with maximum $Index_1$ and $Index_3$ are the voltage key bus in system.

$Index_1$ of each bus is listed in Table 4.1.

Table 4.1

Bus 1	Bus 2	Bus 3	Bus 4	Bus 5
Infinite Bus	2.2906	2.9503	4.2664	4.3755
Bus 6	Bus 7	Bus 8	Bus 9	Bus 10
1.2623	2.0272	2.4756	2.8340	2.6751
Bus 11	Bus 12	Bus 13	Bus 14	Bus 15
4.0628	4.5080	4.2405	4.6465	4.7378

Bus 16	Bus 17	Bus 18	Bus 19	Bus 20
4.5384	4.5920	5.0458	5.0769	4.9912
Bus 21	Bus 22	Bus 23	Bus 24	Bus 25
4.7233	4.7490	5.0174	5.0751	5.2359
Bus 26	Bus 27	Bus 28	Bus 29	Bus 30
5.7279	4.8746	3.1387	5.5009	5.6647

$Index_3$ of each bus is listed in Table 4.2.

Table 4.2

Bus 1	Bus 2	Bus 3	Bus 4	Bus 5
Infinite Bus	0.0851	0.1125	0.2819	0.1926
Bus 6	Bus 7	Bus 8	Bus 9	Bus 10
0.0694	0.1314	0.1662	0.1898	0.1781
Bus 11	Bus 12	Bus 13	Bus 14	Bus 15
0.2819	0.3617	0.1926	0.3843	0.4635

Bus 16	Bus 17	Bus 18	Bus 19	Bus 20
0.3627	0.3947	0.6327	0.6557	0.6067
Bus 21	Bus 22	Bus 23	Bus 24	Bus 25
0.4727	0.4838	0.6241	0.6742	0.7219
Bus 26	Bus 27	Bus 28	Bus 29	Bus 30
1.0643	0.4888	0.2522	0.7680	0.7843

As can be seen, bus 26, 29 and 30 have the maximum absolute value, which mean power change in these buses can have a significant influence on system's voltage. Therefore, bus 26, 29 and 30 can be included in candidate buses.

4.2 **Candidate Bus from Generator Control Constraint**

Generator control constraint is to check whether generators can withstand the real power change brought by wind power dropping and ESS reacting. To diminish the effect of wind power drop on a certain generator, ESS should be allocated in places that can effectively reduce the generator real power output. For example, if a generator is in bus 1, equation (2.21) can be used to determine the voltage angle and magnitude change in system brought by ESS power change. Then, equation 4.6 can be used to calculated real power change in bus 1 (generator bus).

$$\Delta P_1 = \frac{\partial P_1}{\partial \delta_1}\Delta\delta_1 + \frac{\partial P_1}{\partial \delta_2}\Delta\delta_2 + \frac{\partial P_1}{\partial \delta_3}\Delta\delta_3 + \cdots \frac{\partial P_1}{\partial |V_1|}\Delta|V_1| + \frac{\partial P_1}{\partial |V_2|}\Delta|V_2| + \frac{\partial P_1}{\partial |V_3|}\Delta|V_3| + \cdots \tag{4.6}$$

Values listed in Table 4.3 show the influence on generator 1 brought by the 1 per unit real power change in each bus.

Table 4.3

Bus 1	Bus 2	Bus 3	Bus 4	Bus 5
-1.0000	-3.4569	-2.2033	-1.9491	-1.7672
Bus 6	Bus 7	Bus 8	Bus 9	Bus 10
-1.1549	-1.2989	-1.6087	-1.9910	-2.6154
Bus 11	Bus 12	Bus 13	Bus 14	Bus 15
-1.9491	-1.9252	-1.7672	-1.8202	-1.8484

Bus 16	Bus 17	Bus 18	Bus 19	Bus 20
-1.8491	-1.9093	-1.9065	-1.9325	-1.9322
Bus 21	Bus 22	Bus 23	Bus 24	Bus 25
-1.9469	-1.9456	-1.9068	-1.9669	-2.0045
Bus 26	Bus 27	Bus 28	Bus 29	Bus 30
-2.0453	-2.0110	-2.0463	-2.0724	-2.1150

Since the absolute value of bus 2 is the largest, which means its real power change can significantly diminish the power change in generator 1. Therefore if our purpose is to protect

generator 1, our best choice is to locate ESS in bus 2.

Bus 2 can be combined with bus 26, 29, 30 to form 4 candidate buses.

If the generator is located in bus 6, same method can be applied to calculate the influence on generator 6 brought by 1 per unit real power change in each bus.

Table 4.4

Bus 1	Bus 2	Bus 3	Bus 4	Bus 5
Infinite Bus	-2.2629	-4.2841	-11.1845	-4.7922
Bus 6	Bus 7	Bus 8	Bus 9	Bus 10
0.7521	-3.4247	-3.8133	-4.0183	-3.4511
Bus 11	Bus 12	Bus 13	Bus 14	Bus 15
-6.7449	-5.8528	-4.7922	-4.9931	-5.1220

Bus 16	Bus 17	Bus 18	Bus 19	Bus 20
-5.2731	-5.6946	-5.4571	-5.6345	-5.6920
Bus 21	Bus 22	Bus 23	Bus 24	Bus 25
-5.8412	-5.8167	-5.3436	-5.5949	-5.3120
Bus 26	Bus 27	Bus 28	Bus 29	Bus 30
-5.4110	-5.0996	-4.8970	-5.2396	-5.3367

In order to protect generator 6, the best choice is to locate ESS in bus 4.

As voltage key bus in system does not change, candidate bus in this case is bus 4, 26, 29 ,30.

5 Case Study

In the following case study, two different searching space reduction methods are used for determining the candidate bus. Result shows that the first method explained in chapter 4 is more effective in finding candidate bus. After that, different generator location cases are studied. Assuming wind power bus is in bus 3, and generator is located in bus 1, bus 6 and bus 10, among which wind power drop has a significant effect on generator 1 and 6, but has little effect on generator 10. At last, multi-generation system (generator 1 and generator 6) is also studied.

IEEE 30 System is used in the case study with some modification.

①Bus 2 is changed from PV bus to PQ bus.

②The voltage of bus 5, 8, 11, 13 (PV bus) in the system is separately 1.01, 1.02, 1.01, 1.02.

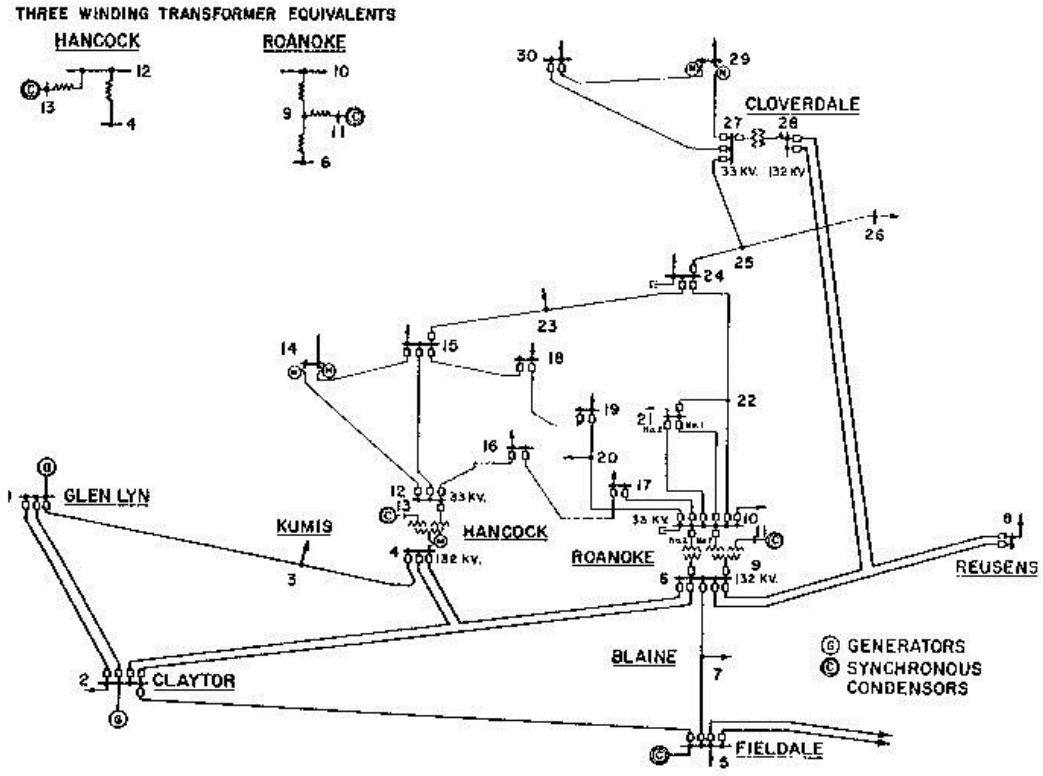

Figure 5.1 IEEE 30 system

Assume there is a 260MW generator in bus 1, and 40 MW wind power generator in bus 3. 3 ESS are planned to be located in this system with constraints, $\alpha = 6.5\%, \beta = 10\%$.

As is explained before, the candidate bus to locate ESS when generator in bus 1 is bus 2, 26, 29, 30. Assuming the wind drop in bus 3 is 50% (20MW), and after 100 tests (each time PSO selects 3 buses from candidate bus and optimize ESS size), it shows the best choice is to locate ESS in bus 2, 26, 30.

If the location of ESS is determined, its size can be calculated by PSO when wind drop changes. Figure 5.2 shows ESS size versus wind drop percentage.

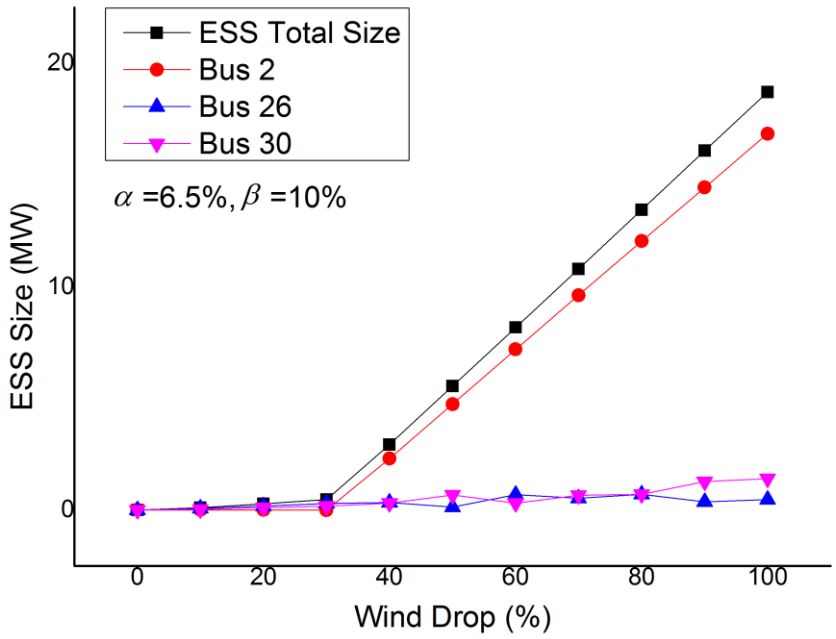

Figure 5.2 ESS size versus wind drop percentage for case 1

It can be concluded from Figure 5.2 that

①ESS total size is growing when wind drop percentage increases.

②There is an obvious turning point in wind drop percentage 30%. Before the turning point, ESS size is mainly concentrated on bus 26 and bus 30. Because, the main constraint before

turning point is the voltage deviation constraint, locating ESS in voltage key buses will help to satisfy the voltage deviation constraint, and save ESS total cost.

③After the turning point, ESS size in bus 2 increases sharply, and so is the ESS total size. Because the main constraint has changed from voltage deviation constraint to control constraint in bus 1. In order to diminish the disturbing in bus 1, bus 2 should output more real power.

④Although after turning point, ESS size mainly increases in bus 2, however, ESS in bus 26 and bus 30 also increase gradually, for larger wind drop will also cause larger voltage deviation, and bus 26 and 30 should generate more real power to satisfy the voltage deviation constraint.

Figure 5.3 shows ESS total size with different control constraint in generator 1.

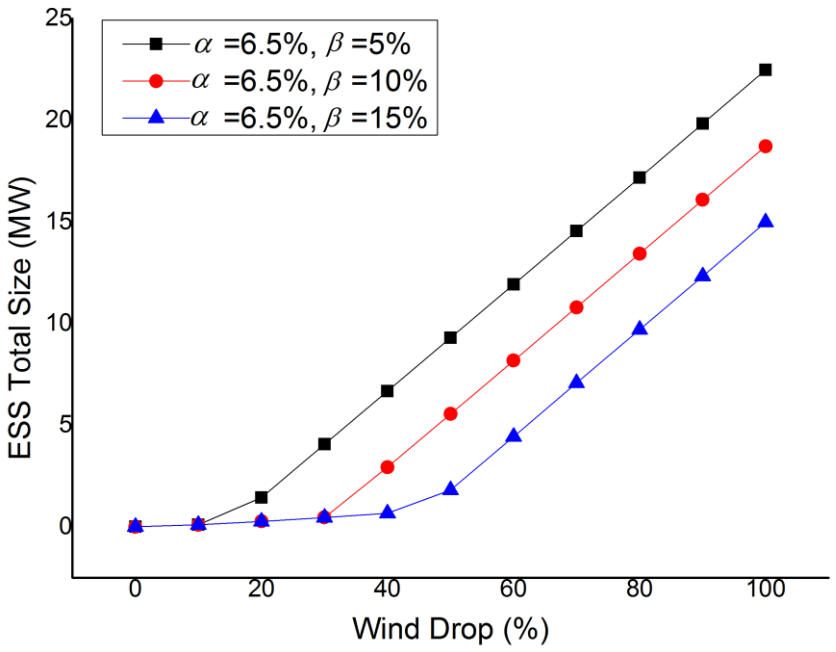

Figure 5.3 ESS total size with different control constraints for case 1

It can be concluded that,

①The stricter the control constraint, the larger ESS total size.

②Plot after the turning point is almost a straight line. Because after the turning point, ESS total

size is mostly increasing in bus 2, and 1 per unit real power change in bus 2 will help to decrease 3.4569 per unit real power change in bus 1, which is a constant. Therefore, when the control constraint for generator 1 is fixed, size in bus 2 will be proportional to the wind drop percentage.

5.1 Contrast with Other Method

The searching space reduction method explained in chapter 4 is also compared with other method. For example, placing ESS at buses that have the largest real power change when wind power changes.

For example, if wind turbine is still in bus 3 and generator in bus 1, equation (2.21) and (2.22) can be used to calculated real power change brought by 1 per unit real power drop in bus 3. The result is listed in table 5.1.

Table 5.1

Bus 1	Bus 2	Bus 3	Bus 4	Bus 5
2.2033	-1.2219	-1.8278	-0.5733	-0.2561
Bus 6	Bus 7	Bus 8	Bus 9	Bus 10
4.2841	-0.0552	-0.7127	-0.4564	0.2457
Bus 11	Bus 12	Bus 13	Bus 14	Bus 15
0.0144	-0.1451	0.0692	0.0300	0.0573

Bus 16	Bus 17	Bus 18	Bus 19	Bus 20
0.0390	-0.0843	-0.0000	0.0000	-0.0320
Bus 21	Bus 22	Bus 23	Bus 24	Bus 25
-0.0889	-0.0437	-0.0000	0.0000	0.0000
Bus 26	Bus 27	Bus 28	Bus 29	Bus 30
0	0.0000	-1.3092	0.0000	0.0000

As can be seen, bus 1 and bus 6 have the largest real power change.

However, because bus 1 is swing bus, which means it is a real power infinite bus, therefore, we can omit bus 1. Combined with system's voltage key bus and wind power bus, there are 5

candidate buses in total, bus 3, 6, 26, 29, 30.

Extensive tests show that the best choice for ESS location in 50% wind drop case is bus 3, 26, 30.

For the ESS locating in bus 3, 26, 30 under constraint $\alpha = 6.5\%$, $\beta = 10\%$, Figure 5.4 shows its total size versus wind drop percentage, in contrast to that of ESS in bus 2, 26, 30.

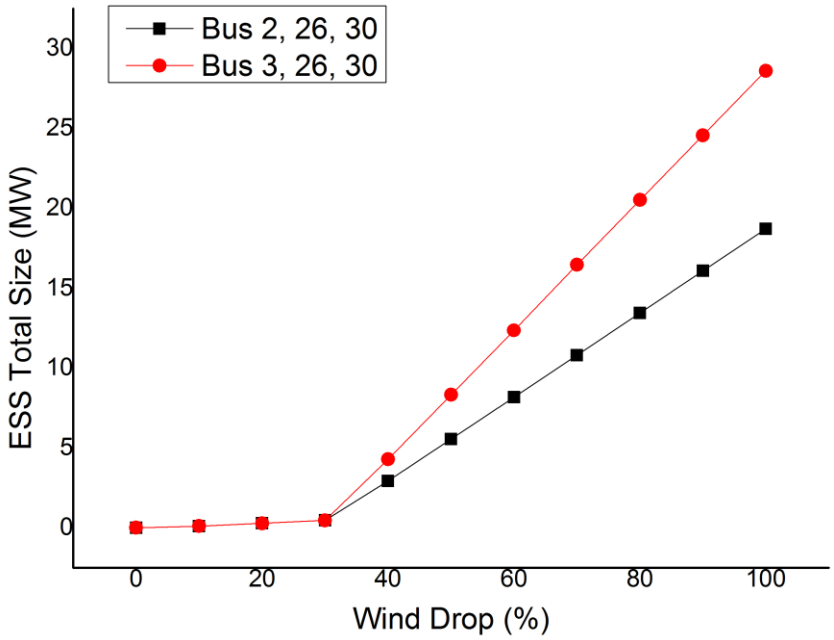

Figure 5.4 ESS total size versus wind drop percentage

It can be seen that ESS in bus 3, 26, 30 will need more ESS size than that in bus 2, 26, 30 to satisfy the same voltage and control constraint. Hence, the first candidate bus searching method can find more effective buses to locate ESS that not only diminishes the disturbance on generator bus but also maintain system voltage profile when wind power drops.

Similarly, if the generator is moved to bus 6, the same conclusion can be drawn that the first method is better for choosing candidate bus for ESS. When wind drop increases to 100%, the second method will cost almost as 2 times total ESS size as the first method.

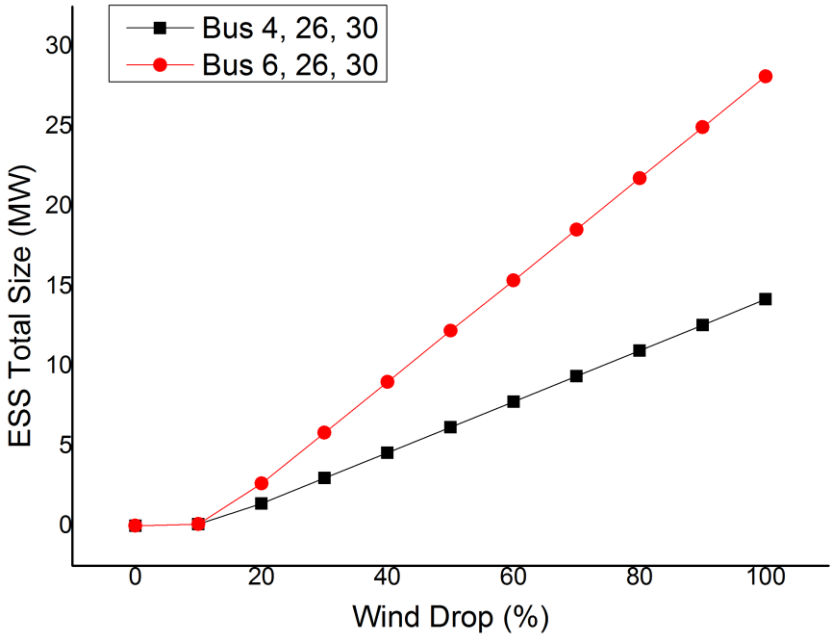

Figure 5.5 ESS total size versus wind drop percentage

5.2 Impact of Generator Location

Different generator location will result in different ESS location and size. The case study here assumes wind power bus is in bus 3, and generator is moved to different locations.

5.2.1 Generator in bus 6

As is calculated in chapter 4, if generator is moved to bus 6 whose rated power is 200MW, candidate bus will be bus 4, 26, 29, 30.

Extensive tests show the best choice to locate ESS in 50% wind drop case is bus 4, 26, 30.

Assuming ESS is located in bus 4, 26, 30, Figure 5.6 shows ESS size versus wind drop changes under constraint $\alpha = 6.5\%, \beta = 10\%$

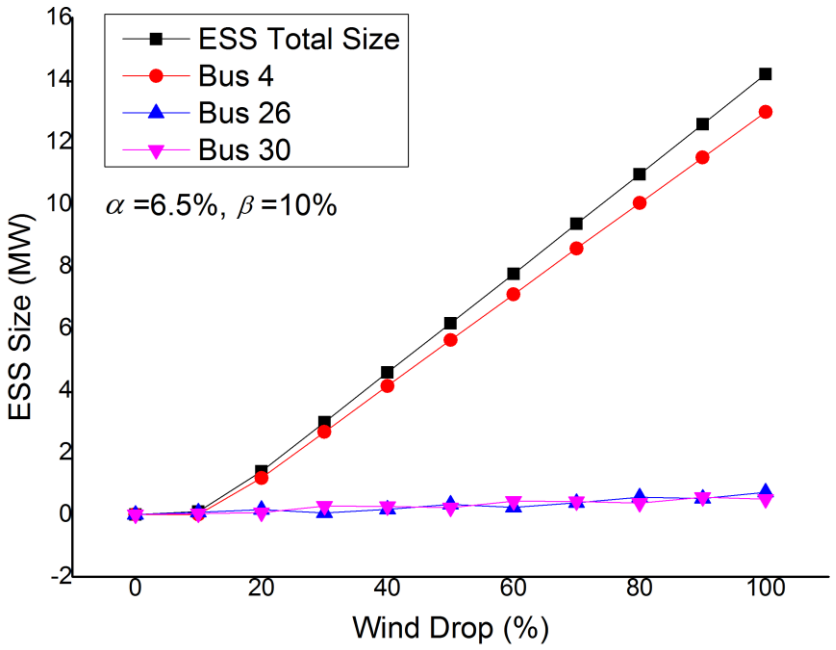

Figure 5.6 ESS size versus wind drop percentage for case 2

Figure 5.7 shows ESS total size with different control constraints in generator 6.

Compared to Figure 5.3, Figure 5.7 has almost the same regulation. However, the ESS total size is smaller than that in Figure 5.3.

Because as is listed in Table 4.3 and Table 4.4, one per unit real power change in bus 4 causes -11.1845 per unit real power change in generator 6 while one per unit real power change in bus 2 only cause -3.4569 per unit change in generator 1. Therefore, with the same constraint, ESS in bus 4 can have a smaller size than that in bus 2, resulting in smaller ESS total size.

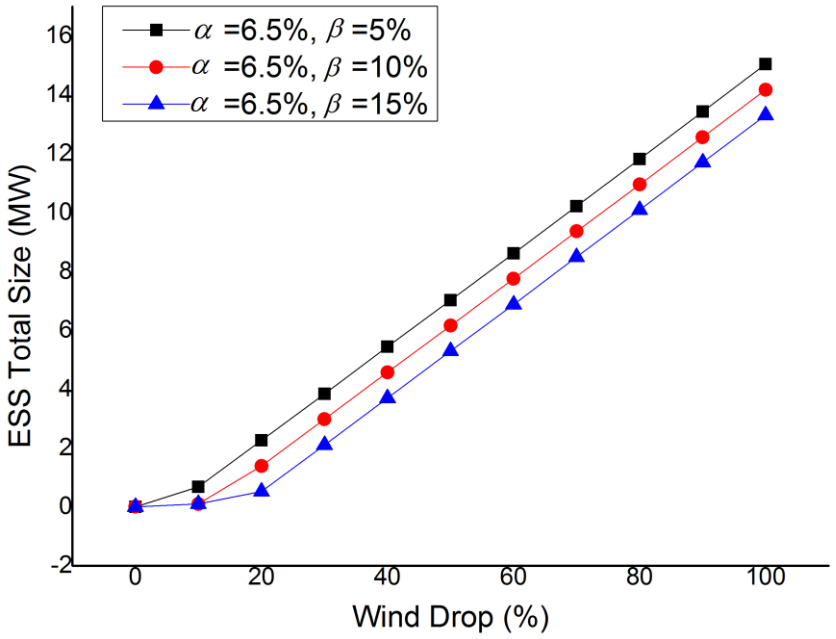

Figure 5.7 ESS size with different control constraints for case 2

5.2.2 Generator in Bus 10

If the 200 MW generator is moved to bus 10, table 5.2 shows the influence on generator 10 brought by one per unit real power change in each bus

Table 5.2

Bus 1	Bus 2	Bus 3	Bus 4	Bus 5
Infinite Bus	1.8931	-0.2457	-2.6383	-2.4998
Bus 6	Bus 7	Bus 8	Bus 9	Bus 10
0.1334	-0.3210	-0.3963	-0.2056	2.6969
Bus 11	Bus 12	Bus 13	Bus 14	Bus 15
-2.6383	-3.9353	-2.4998	-2.7933	-3.0418

Bus 16	Bus 17	Bus 18	Bus 19	Bus 20
-3.5561	-4.5257	-3.7672	-4.1836	-4.3750
Bus 21	Bus 22	Bus 23	Bus 24	Bus 25
-4.7547	-4.6794	-3.3652	-3.7679	-2.4756
Bus 26	Bus 27	Bus 28	Bus 29	Bus 30
-2.5350	-1.6537	-0.3858	-1.7299	-1.7828

In order to diminish the disturbance brought by wind drop, the best choice is to locate ESS in bus 21. Combined with voltage key bus 26, 29, 30, there are 4 candidate buses in total. After extensive tests, it shows that the best location for allocating ESS in 50% wind drop case is bus 4, 26, 30.

Figure 5.8 shows ESS size when wind drop changes, $\alpha = 6.5\%, \beta = 10\%$.

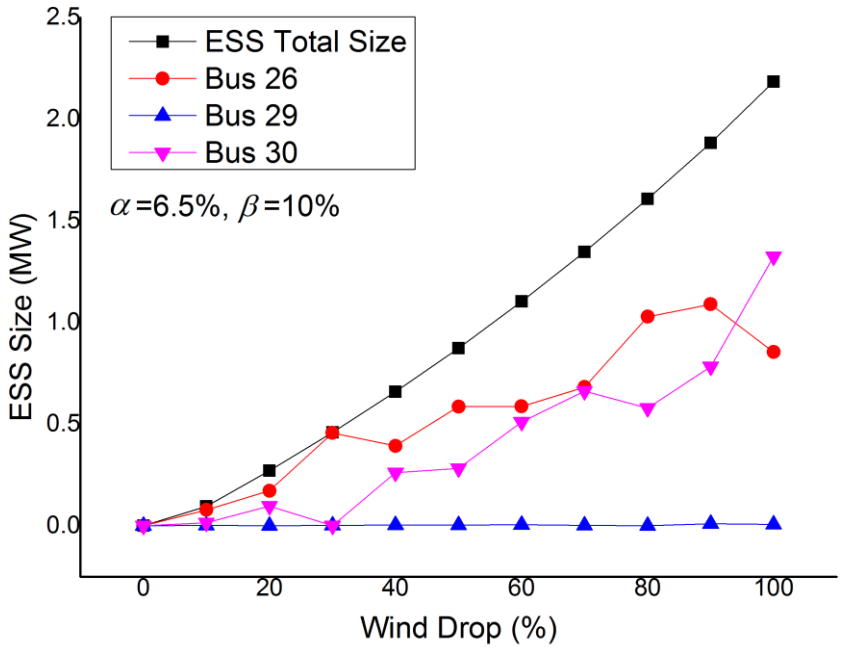

Figure 5.8 ESS size versus wind drop percentage for case 3

As can be seen, the total ESS size is much smaller than former cases because wind drop in bus 3 has little effect on generator 10. Most of the ESS size is in bus 26 and bus 30, which are more sensitive than bus 29 to system's voltage according to table 4.1 and table 4.2.

Since generator size is too large, even wind power drops 100%, has little effect on generator 10. Therefore, the control constraints will always be loose and ESS total size will be essentially the same when control constraint varies.

If the rated power of generator 10 is changed to 40MW, and control constraint remains

unchanged, the best candidate bus combination will be changed to bus 21, 26, 30.

Figure 5.9 shows ESS size versus wind drop under constraint $\alpha = 6.5\%, \beta = 10\%$

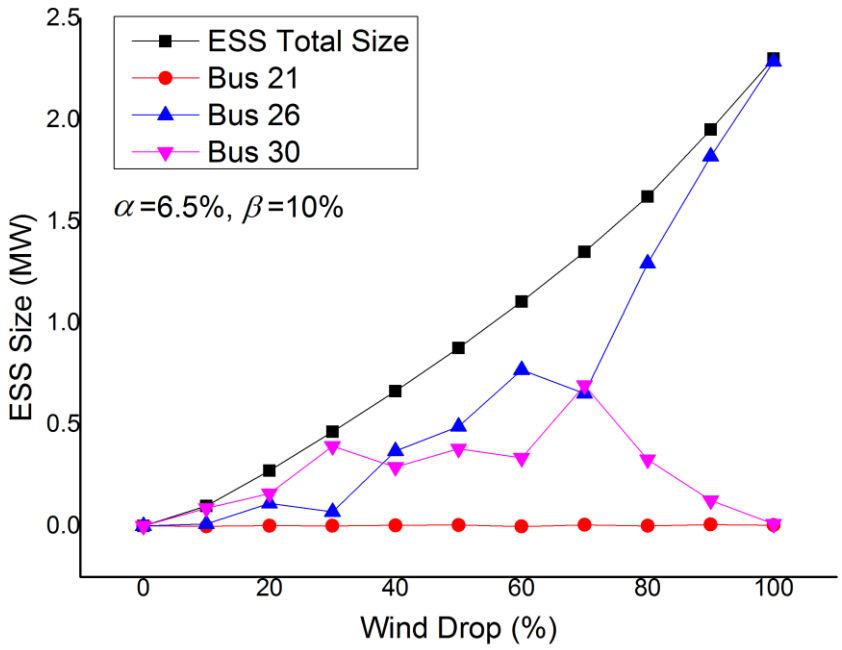

Figure 5.9 ESS size versus wind drop percentage for case 3

In Figure 5.9, most of ESS capacity is located in bus 26, which is not only the voltage key bus in system, bus also an effective protector for generator 10.

Figure 5.10 shows ESS total size for different control constraints in generator 10. Curve that represents ESS total size when generator's rated power is 200MW is also added as a comparison.

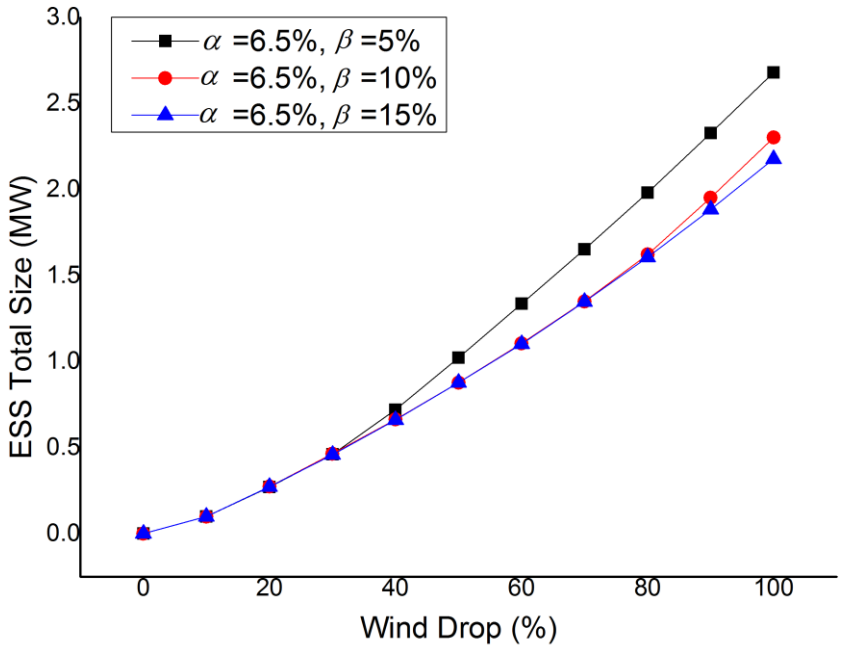

Figure 5.10 ESS total size with different control constraint for case 3

It can be concluded that,

①The stricter the constraint, the larger ESS total size.

②When wind drop is low, three cases have the same ESS total size. Because when wind drop is low, it will bring little disturbance on generator 10 which is smaller than the control constraint. Only voltage constraint will work. Since voltage constraints for each case is 10%, therefore three cases have the same ESS total size.

③When wind drop increases, black, red and blue lines will have a different ESS size. Black line deviates from blue line when wind drop reaches 30% and red line deviates when wind drop reaches 60%.

5.2.3 Generator in Bus 1 and Bus 6

If there are two generators in the system, one in bus 1 and the other in bus 6, the candidate bus

will change to bus 2, 4, 26 and 30.

50% wind drop case study shows that the best locations for ESS are bus 2, 4, 26.

Assuming ESS are located in these buses, Figure 5.11 shows ESS size in each bus versus wind drop changes, under constraints $\alpha = 6.5\%$, $\beta = 10\%$.

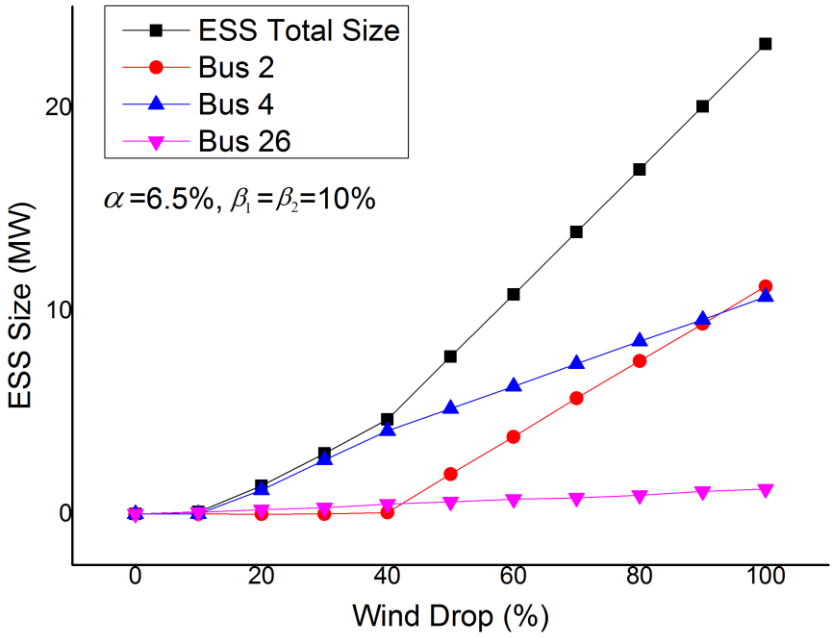

Figure 5.11 ESS size versus wind drop percentage for case 4

There are two obvious turning point of ESS total size in Figure 5.11. The first turning point is caused by turning point of bus 4, and the second turning point is caused by turning point of bus 2. Although ESS size in bus 2 is initially smaller than that in bus 4 at low wind drop, it then sharply goes up and finally exceeds that in bus 4.

Since, one per unit drop in bus 3 will cause 2.2033 per unit real power change in bus 1, and 4.2841 per unit real power change in bus 6. In other word, wind power drop will have a more significant influence in generator 6. When the wind drop is low, it causes little effect on bus 1, which is smaller than the control constraint for generator 1, so ESS size in this case is smaller.

However, as listed in Table 4.3 and Table 4.4, one per unit real power change in bus 4 causes -11.1845 per unit change in generator 6 while one per unit real power change in bus 2 only cause -3.4569 per unit change in generator 1, which means ESS in bus 4 can has stronger effect on the real power change in generator 6. Therefore, the ramp rate of ESS size in bus 4 is smaller. Besides, bus 26 will gradually increase to satisfy the voltage constraint in system.

6 Verification of the Proposed Algorithm

Since ESS planning is only based on some specific wind power cases, it is important to verify if this planning can handle of all the cases, especially when wind drop is low.

For instance, if generator is in bus 1, the ESS planning case is wind drop 50% with constraint $\alpha = 6.5\%, \beta = 10\%$.

PSO optimization result is shown in Table 6.1.

Table 6.1

Bus Number	Size (MW)
Bus 2	4.734393
Bus 26	0.131776
Bus 30	0.678929

Table 6.2 shows the voltage deviation and generator disturbing in different wind power drop case.

Wind drop (%)	Voltage deviation (%)	Disturbing to generator (%)
0	6.29	-6.95
10	6.33	-3.56
20	6.37	-0.17
30	6.41	3.22
40	6.45	6.61
50	6.50	10.00
60	6.55	13.39
70	6.61	16.78
80	6.66	20.17
90	6.72	23.56
100	6.79	26.95

If generator is in bus 6, the ESS planning case is wind drop 50% with constraint $\alpha = 6.5\%, \beta = 10\%$.

Table 6.3 shows PSO optimization result.

Table 6.3

Bus Name	Size (MW)
Bus 4	5.615464
Bus 26	0.323118
Bus 30	0.217879

Table 6.4 shows the voltage deviation and generator disturbance in different wind power drop cases.

Table 6.4

Wind drop (%)	Voltage deviation (%)	Disturbing to generator (%)
0(ESS in bus 4 output 1 MW)	6.35	-7.10
10(ESS in bus 4 output 1 MW)	6.38	1.52
20(ESS in bus 4 output 2 MW)	6.41	4.50
30	6.41	-7.15
40	6.45	1.41
50	6.50	9.98
60	6.55	18.55
70	6.60	27.12
80	6.65	35.69
90	6.71	44.26
100	6.77	52.82

It can be concluded, 50% wind drop planning can handle all the cases when wind power suddenly drops less than 50%, since the voltage deviation constraint and generator control constraint can both be satisfied. Sometimes, ESS in some buses should output less real power than scheduled, otherwise generator will absorb too much real power, which is also a severe disturbance.

50% wind drop planning cannot handle any case when wind drop is more than 50% as generator should output too much real power and also the voltage deviation of system is too large.

7 Conclusion and Future Work

- In this research, control factor is integrated into ESS planning. Sensitivity analysis is used to linearize the real power change in a certain generator caused by wind and ESS power change in the system. PSO is modified to include the real power change percentage as a constraint, and used to determine optimum ESS size and location. After extensive tests, it shows that this method can determine the right sizes and locations for ESS, which can effectively diminish the disturbance on generators in system as well as maintaining the acceptable system voltage profile after a sudden voltage drop.
- Sensitivity analysis is also applied to choose candidate bus for ESS planning. Candidate bus can be grouped into two categories, system voltage key bus and generator control key bus, in which the former is associated with system structure, and the latter is related to generator and wind farm location.
- Next step is to include more detailed parameters in generator transient process so that ESS allocation optimization can be integrated with accurate real time control information in planning.
- Real time PSCAD simulation is needed to verify the planning result.
- Since the planning is based on specific wind drop case but wind power distribution is statistic. It is necessary to include the statistic planning method in optimization.

8 References

[1] G. W. E. Council. (2014). Global Wind Energy Outlook 2014 [Online]. Available: http://www.gwec.net/wp-content/uploads/2014/10/GWEO2014_WEB.pdf.

[2] KejunQIAN, Chengke ZHOU, Zhaohui LI, YueYUAN. "Benefits of Energy Storage in Power System with High Level of Intermittent Generation", 20th International Conference on Electricity Distribution.

[3] S. Wen, H. Lan, Q. Fu, D. C. Yu, "Economic allocation for energy storage system considering wind power distribution", IEEE Transaction on Power System, vol. 30, pp. 644-652, 2015.

[4] Peng Xiong, Chanan Singh, "Optimal Planning of Storage in Power Systems Integrated With Wind Power Generation", IEEE Transaction on Sustainability Energy, vol. 7, pp. 232-240, 2016.

[5] Z. Y. Gao, P. Wang, L. Bertling, J. H. Wang, "Sizing of energy storage for power systems with wind farms based on reliability cost and wroth analysis", IEEE Power and Energy Society General Meeting. pp. 1-7, 2011.

[6] Luis Fernando Montoya Sanchez, "Novel methodology to determine the optimal energy storage location in a microgrid to support power stability", The University of Wisconsin-Milwaukee, December 2012.

[7] Grainger & Stevenson, Power System Analysis, Electrical and Computer Engineering Series, 1st edition.

[8] Adriano Aron F. de Moura, Ailson P. de Moura, "Newton-Raphson decoupled load flow with constant matrices of condutance and susceptance", 2010 9th IEEE/IAS International

Conference on Industry Applications. pp. 1-6, 2010.

[9] Particle Swarm Optimization: Tutorial, http://www.swarmintelligence.org/tutorials.php, Mar. 28, 2016.

[10] Youcef Amrane, Mohamed Boudour, Messaoud Belazzoug, "Optimal Reactive Power Planning based on Particle Swarm applied to the Algerian Electrical Power System", 2013 3rd International Conference on Systems and Control (ICSC), pp. 804-809, 2013.

[11] Y.Amrane, M.Boudour, "Particle swarm optimization based reactive power planning for voltage stability improvement", 2014 International Conference on Electrical Sciences and Technologies in Maghreb (CISTEM), pp. 1-7, 2014.

[12] IEEE 30 System, https://www.google.com/search?q=IEEE+30&espv=2&biw=1366&bih=667&tbm=isch&tbo=u&source=univ&sa=X&ved=0ahUKEwi5_JyT3fDLAhVGIJoKHRZWC9cQsAQIGw#imgrc=NrkGOMTYCOb9vM%3A, Apr. 1, 2016.